Article:
Miranda, Juliana Fabiani, Rogerson, Adam, Guthrie, Megan et al. (6 more authors) (2025) Ex vivo modelling reveals low levels of CKS1 inhibition boost haematopoiesis via AKT/Foxo1 signalling. Experimental hematology. 104768. ISSN 0301-472X

https://doi.org/10.1016/j.exphem.2025.104768

***Title*: *Ex vivo* modelling reveals low levels of CKS1 inhibition boost haematopoiesis via AKT/Foxo1 signalling.**

Authors: Juliana Fabiani Miranda[1], Adam Rogerson[1], Megan Guthrie[1], Kimrun Kaur[1], Emma Apperley[1], Mary Catherine Dunne[1], Navin Shridokar[1], Anjum Khan[1,2], William Grey[1*].

1. ProteoStem lab, Centre for Blood Research, York Biomedical Research Institute, University of York, York, U.K
2. Department of Haematology, Leeds Teaching Hospitals NHS Trust, Leeds, U.K.

* correspondence: William.grey@york.ac.uk

+447595502484

Department of Biology

University of York

Wentworth Way

York

YO10 5DD

United Kingdom

Category for table of contents

Normal Hematopoiesis

Stem Cells (secondary category)

Word count

3,989

Abstract

Hematopoietic stem cells (HSCs) are rare cells residing at the top of the haematopoietic hierarchy capable of reconstituting all blood cell populations through their ability of self-renewal and differentiation. Their ability to maintain haematopoiesis can be majorly depleted by chemotherapeutic agents, leading to a long-term bone marrow injury. However, pre-clinical studies have focused on the acute effects of chemotherapy, leaving the lasting impact on healthy cells poorly understood. To study this, we combined rapid *ex vivo* models to study the long-term/late-stage effects of a cyclin-dependent kinase subunit 1 (CKS1) inhibitor. Inhibition of CKS1 has been shown to protect healthy HSCs from chemotherapy during acute myeloid

leukaemia, and here we show a dose-dependent role of long-term CKS1 inhibition on haematopoiesis, either boosting B lymphopoiesis or ablating HSC proliferation capacity, dependent on the context. Mechanistically, low doses of the CKS1 inhibitor (CKS1i) affects AKT-Foxo1 signalling potentiating B-cell differentiation, but impairing HSC proliferation. These results reveal a novel role for CKS1 in boosting B lymphopoiesis and propose the use of rapid *ex vivo* models to investigate the long-term effects of chemotherapeutic treatments targeting HSCs with the potential of reducing late adverse effects.

Introduction

Hematopoietic stem cells (HSCs) reside at the top of the hematopoietic hierarchy and generate around 90% of the total cells in our bodies. This is possible due to two main characteristics: self-renewal and differentiation, both crucial for maintaining hematopoietic homeostasis[1]. The hematopoietic system is highly sensitive to systemic chemotherapy, thus, studying HSC expansion and differentiation is important when developing novel therapies. However, the underlying mechanisms of HSC maintenance, expansion and differentiation are not always fully understood in response to novel chemotherapeutic agents due to their paucity in primary tissue and historically the lack of robust *ex vivo* culture systems to study this cell population.

Pre-clinical studies of novel agents targeting haematological disorders mainly focus on the malignant cells, with limited testing of systemic short-term or long-term effects on healthy tissue prior to early-stage clinical trials. Whereas HSCs have been shown to be more resistant to therapeutic treatments than other blood cells due to their quiescence, patients can develop a long-term bone marrow (LT-BM) injury affecting HSC reserves and functionality, consequently affecting the whole hematopoietic system. LT-BM damage generally fails to recover, has severe effects on quality of life due to infection risk and transfusion burden, and can develop into life-threatening disorders such as aplastic anaemia, bone marrow failure and myelodysplastic syndromes[2]. Furthermore, conventional frontline treatments such as cytarabine plus doxorubicin demonstrate well documented acute toxicities, including mortality, and long-term effects on HSCs[3–5]. Similarly newer therapies such as Venetoclax have made major inroads in treating frailer patients, but haematological toxicity and limited longer term efficacy have reduced the scale of clinical benefit, particularly in adverse risk patients[6,7]. Thus, understanding and mitigating the sustained damage of chemotherapy on healthy HSCs can help increase treatment efficacy and reduce lasting side-effects. In this study, we focus on understanding long-term/late-stage effects on LT-HSCs and their progeny, using a small

molecule inhibitor targeting the cyclin-dependent kinase subunit 1 (CKS1) that has been shown to play a crucial role in regulating both HSC homeostasis and cancer development[8–10].

CKS1 is known for its associations with CDK and E3 ligase complexes, responsible for regulating phosphorylation and degradation of key haematological factors, including the CDK inhibitor p27[11], mixed lineage leukaemia 1 (MLL1)[10] and activation of RAC1[9]. Importantly, *Cks1* knockout in mouse models resulted in disrupted HSC functionality, abrogating their ability to transplant and reconstitute the hematopoietic system[8,11]. Moreover, we recently demonstrated the dual effects of selective inhibition of the $SCF^{SKP2\text{-}CKS1}$ E3 ligase complex using a small molecule inhibitor (CKS1i) in acute myeloid leukaemia (AML), simultaneously depleting leukemic stem cells (LSCs) whilst preserving healthy HSCs and intestinal stem cells from the acute cytotoxic effects of chemotherapy treatment. Whereas high expression of CKS1 on LSCs makes them an optimal target for CKS1i, its inhibition in healthy HSCs leads to an accumulation of p27 and induced quiescence, preventing DNA integration of chemotherapeutic agents and consequent toxicity[9,10].

These studies showed the critical role of CKS1 in HSC functionality under non-homeostatic conditions. However, this may not mitigate the potential effects of chronic CKS1i treatment – which could have the same outcome as *Cks1*$^{-/-}$ – nor provide information on long-term/late-stage effects on haematopoiesis, which remains an understudied area in novel therapeutic development. This study aims to understand the effects of CKS1i on the intrinsic properties of healthy stem cells under both expansion and differentiation conditions.

Methods

Animals and in vivo inhibitor study

Animal experiments were performed under the U.K. Home Office project license (PP4650015) in accordance with the Home Office (UK). For *in vivo* study, 8-12 week old C57BL/6 wild type mice were treated with CKS1i (10mg/kg) or vehicle control for 5 consecutive days, as per our previous work[9], and, after 2 days interval, peripheral blood cellular composition was assessed for the following 5 days and bone marrow composition was assessed after 3 days by flow cytometry. Blood counts were assessed at days 6, 9 and 11 on a ProcyteDX.

In vitro PVA-based HSC expansion

These experiments were performed according to the original publication[12]. For all expansion experiments, 10 $cKit^{+}Sca1^{+}CD48^{-}CD150^{+}EPCR^{+}Lineage^{-}$ (ESLAM)-HSCs were sorted per well in fibronectin-coated 96-well plates (Fn, 10 µg/cm^2; Sigma) in complete Dulbecco's

Modified Eagle Medium F12 (F12, with 1% P/S, 1% L-glutamine, 10mM HEPES, 1mg/ml polyvinylalcohol – PVA, and 1% insulin-transferrin-selenium ethanolamine, Thermo Fisher Scientific) supplemented with thrombopoietin (TPO, 100ng/ml; Peprotech), stem cell factor (SCF, 10 ng/ml; Peprotech) and treated or not (control) with CKS1i (Sigma-Merck) from day 0 or day 5 in culture. Full media changes were performed three times a week starting from day 7 without disrupting the Fn-layer. At day 21, populations were immunophenotyped by flow cytometry.

In vitro multilineage differentiation

These experiments were performed according to the original publication[13]. For all co-culture experiments, 10 ESLAM-HSCs were sorted per well in a 96-well plate containing OP9 stromal cells at 80% confluency in complete Opti-MEM supplemented with FMS-like tyrosine kinase 3 ligand (Fl3tl) (50 ng/ml; Peprotech), SCF (50 ng/ml; Peprotech) and treated with CKS1i at dose escalation concentrations indicated. At day 4, ESLAM-HSCs were harvested, and half the cells were seeded into the “B-lymphopoiesis condition” with a new OP9 stromal cell layer in complete Opti-MEM supplemented with Flt3L, SCF and interleukin-7 (IL-7) (20 ng/ml; Proteintech Europe), and the other half of cells seeded in monoculture in the “Erythro-myelopoiesis condition” with StemSpan SFEM I (StemCell Technologies) supplemented with Flt3L, SCF, holo-transferrin (HT, 0.3 mg/ml; Merck Life Scientific) and erythropoietin (EPO, 3 U/ml; StemCell Technologies), with or without (control) CKS1i treatment. Half media changes were performed twice per week and, at day 21, populations were immunophenotyped by flow cytometry.

Proteomic sample preparation and analysis

Primary cKit^{+}Sca1^{+}Lineage^{-} (LSK) cells were grown in co-culture with OP9 stromal cells in complete Opti-MEM supplemented with Flt3L and SCF and treated or not (control) with CKS1i (1 µM) for 4 days. Cells were harvested and 50,000 CD45^{+} cells were sorted per sample using a MoFlo Astrios sorter for proteomic analysis. Cells were lysed using urea lysis buffer and sonication and digested overnight in urea digestion buffer. Protein extract was loaded onto Evotips (Evosep) and measured on a timsTOF HT (Bruker). Liquid chromatography-mass spectrometry data were searched by data independent acquisition (DIA)-NN software (Cambridge) against the mouse reference (Supplementary Table 2).

Results

Acute CKS1i treatment has no effect on haematopoietic homeostasis *in vivo*

To study the acute effects of CKS1 inhibition on haematopoietic homeostasis we treated wild-type mice with CKS1i[9] and measured peripheral blood cellular composition and total blood cell counts (Fig. 1a and Suppl. Fig. 1a, b). We observed no significant difference in blood cell counts (Suppl. Fig. 1b) and mature blood populations between vehicle control and CKS1i-treated mice across erythroid, myeloid and lymphoid cell types (Fig. 1b-g), and both control and CKS1i-treated mice show a reduction in $Gr1^{-}CD11b^{+}$ monocytes 11 days after treatment commenced, 4 days after the initial peripheral blood sample (Fig. 1f). Bone marrow composition analysis (Suppl. Fig. 1c) showed no difference in primitive hematopoietic population cell numbers under CKS1i-treatment (Fig. 1h-r). We also observed that CKS1i decreased total live cell numbers within the bone marrow (Suppl. Fig. 1e). Whereas most primitive cell populations showed no difference in proportion between control and CKS1i-treated mice (Suppl. Fig. 1e-n), proportion of HSC and ESLAM-HSC increased upon CKS1i-treatment (Suppl. Fig. 1o, p), agreeing with previous observations in *Cks1-/-* mice[8] and CKS1i treated AML PDX[9]. Together these results demonstrate that acute treatment with CKS1i does not affect haematopoietic homeostasis immediately after administration.

CKS1i ablates ESLAM-HSC proliferation capacity in vitro

To initially study the ability of ESLAM-HSCs to expand under increasing doses of CKS1i (0 - 20 µM), we used the PVA-based murine HSC expansion system[12]. We analysed the ability of ESLAM-HSCs to expand, maintain immunophenotypic haematopoietic stem and progenitor cells (HSPCs) and produce differentiated cell types (Suppl. Fig. 2a).

ESLAM-HSCs were treated with CKS1i from day 0 or allowed to recover in culture and treated from day 5, and grown for 21 days in the PVA culture system (Fig. 2a). Our analysis of megakaryocyte, myeloid and primitive ($CD11b^{-}Gr1^{-}$) populations (Suppl. Fig. 2a) showed that, if treated at day 0, even the lowest doses of CKS1i deplete primitive cells in 21-day expansion cultures (Fig. 2b). When allowed 5 days to recover and begin to proliferate before treatment with CKS1i, cells were able to grow under treatment concentrations up to 0.1 µM (Fig. 2b). However, total expansion potential of primitive fractions (LSK, $cKit^{+}Sca1^{+}Lineage^{-}$) under 0.1 µM treatment was still reduced when compared to control (Suppl. Fig. 2b), with no significant difference in the number of more committed progenitors (LK, $cKit^{+}Sca1^{-}Lineage^{-}$) (Suppl. Fig. 2c). Furthermore, we observed that 4-days treatment with CKS1i induces apoptosis in $CD45^{+}$ cells at 0.5 µM concentration either treating from day 0 or day 5 in expansion culture (Fig. 2c, d), showing that lower concentrations (0.05uM, 0.1uM) halt proliferation potential of primitive hematopoietic populations without affecting their survival. Interestingly, at 0.5 µM the most

primitive cell population (LSK) is the first to disappear (Fig. 2e, f), indicating that some differentiation occurs but HSPCs are not maintained.

Comparatively, differentiated megakaryocyte progenitors (MKP, cKit$^+$CD41$^+$Lineage$^-$), megakaryocytes (MK, cKit$^-$CD41$^+$Lineage$^-$) (Suppl. Fig. 2d, e), monocytes plus dendritic cells (Mo+DC, CD11b$^+$Gr1$^-$), and granulocytes plus neutrophils (GR+N, CD11b$^+$Gr1$^+$; Suppl. Fig. 2f, g) substantially decrease in numbers at 0.5 µM treatment with CKS1i when compared to control. However, we do not observe significant expansion or lineage skewing amongst the populations analysed (MKP, MK, Mo+DC and GR+N) under CKS1i-treatment within this system. These results suggest that low concentrations of CKS1i completely ablate ESLAM-HSC expansion potential within a highly proliferative system, and that more primitive cell populations such as LSKs have higher sensitivity to CKS1i when compared to mature populations, potentially affecting the differentiation of early progenitor cells.

Inhibition of CKS1-dependent protein degradation reveals lineage-specific differentiation sensitivity

Next, we assessed the effect of CKS1i on differentiation potential of ESLAM-HSCs, applying the Safi et al. *ex vivo* multilineage differentiation protocol[13] (Fig. 3a). Within the first four days we observed increasing apoptosis following gradual CKS1i concentration increase, with a significantly higher percentage of CD45$^+$ apoptotic cells at 5 µM treatment compared to control after 24h or 4 days (Fig. 3b, c). These results show a higher resilience of primitive LSKs to CKS1i when compared to AML cell lines (THP1 and KG1a) IC50 values between 1-2 µM (Suppl. 3a). We have previously shown that CKS1i increases p27 protein inducing cell cycle arrest in human HSCs[9]. In agreement, we observed that CKS1i induces an increase of p27 (Suppl. Fig 3b, c) whilst decreasing Ki67 positive cells and cell numbers (Suppl. Fig 3d-f) of murine LSK cells when compared to control during the first 4 days of culture, showing that, even though LSKs in co-culture with OP9s are less sensitive to CKS1i when compared to expansion culture, cell numbers still decrease due to the anti-proliferative effects of the drug. Furthermore, after 21 days in culture, our results showed the depletion of myeloid (CD45$^+$CD11b$^+$), B lymphoid (CD45$^+$CD19$^+$) and Ter119$^+$ erythroid (CD45$^-$Ter119$^+$) populations (Suppl. Fig. 3g) at stress-inducing/apoptotic CKS1i concentrations (5 to 20 µM, Fig. 3d). Interestingly, low concentrations of CKS1i (0.05 to 1 µM) boost differentiated cell population numbers when compared to controls (Fig. 3d). A slight (non-significant) increase in cell numbers at low doses of CKS1i could be observed within Ter119$^+$ cells and B cells after only 7 days in culture, suggesting a CKS1i-treatment response from early stages of B cells and erythroblast differentiation (Suppl. Fig. 3 h-i). In contrast, CKS1i-treatment does not boost AML cell line numbers in culture (Suppl. Fig. 3j).

200 Under erythropoiesis conditions, Ter119^{+} cell numbers only reduce at 10 µM of CKS1i when
201 compared to controls (Fig. 3e, f). Within the B condition, low doses of CKS1i (0.05 to 0.5 µM)
202 boost B cell numbers in culture, whereas at 1 µM these cells are depleted (Fig. 3g, h).
203 Furthermore, following B lymphopoiesis induction, CD45^{+} immune cells, but not CD45^{-} cells,
204 are broadly depleted when treated with 5 µM of CKS1i (Suppl. Fig. 3k). We investigated
205 whether CKS1i treatment effect on B lymphopoiesis was due to reduction of OP9 stromal cell
206 viability. We observed that OP9s are highly resilient to CKS1i with only reduced viability at 20
207 µM (Fig. 3i), showing that the CKS1i effects within the B condition are independent of OP9
208 cell viability. We also observed that macrophages (Suppl. Fig. 3m, n), as well as myeloid
209 populations (Suppl. Fig. 3o, p) and total live cells (Suppl. Fig. 3q) had lower numbers in culture
210 within the B condition under 1 µM-treatment with CKS1i compared to those in the ER condition.
211 This suggests a cytokine-specific response to CKS1i.

212 **Proteomic analysis of the CKS1i response reveals an AKT/Foxo1-driven alteration in**
213 **primitive cells**

214 To investigate the mechanism underlying the bimodal role of CKS1i within haematopoiesis,
215 and specifically the conditions which boost B lymphopoiesis, we cultured LSKs with 1 µM of
216 CKS1i on OP9 cells and performed total proteomics on sorted CD45^{+} cells (Fig. 4a). When
217 mapped to murine haematopoiesis, our results demonstrated that differentially abundant
218 proteins are more representative of LT-HSCs and pre-B cells, with low representation of pro-
219 Erythrocytes when using CellRadar (Fig. 4b). Interestingly, the differential sensitivities of
220 immune populations to CKS1i do not match the expression profile of *Cks1b* alone in the murine
221 haematopoietic hierarchy (Suppl. Fig 4a, yellow). However, when we mapped the CKS1
222 protein and proteins differentially abundant after CKS1i treatment in human HSCs[9] onto
223 mouse haematopoiesis, our results showed a different lineage bias between CKS1 alone and
224 CKS1i responsive proteins (Suppl. Fig. 4a). Despite cytokine supplementation for human HSC
225 cultures being different and no co-culture layer present, CKS1i responsive proteins in human
226 HSCs were more similar to that seen in our results here.

227 To better understand the mechanism of action leading to increased B lymphopoiesis at low
228 levels of CKS1i treatment, we focussed on a network analysis incorporating the strongest
229 discriminators between untreated control and CKS1i-treated (Fig. 4c, Supp. Fig. 4b-d). Of the
230 proteins significantly altered in CKS1i versus control, and classic CKS1i-targeted proteins,
231 string analysis mapped interactions involved in the regulation of AKT, Foxo1 and NFkB (Fig.
232 4d), such as TAB3, CAT, GSTA4, NRP1, PIR, DPP4 and MUC13 (Suppl. Fig. 4d-f). Our results
233 showed that CKS1i (at 1 and 5 µM) induces AKT phosphorylation (T308) in LSKs when

compared to control (Fig. 4e, f and Suppl. Fig. 4g), as well as increasing total AKT (Suppl. Fig. 4h).

It is known that AKT can regulate the NFkB/IKBa axis[14]. Our results showed an increase in the NFkB/IKBa ratio at 5µM CKS1i concentration (Fig. 4g, h and Suppl. Fig. 4i, j), similar to increased apoptosis previously observed (Fig. 3b, c). However, inhibition of AKT further increases NFkB abundance on LSKs treated with CKS1i (5 µM) when compared to control (Suppl. Fig. 4k, l). Together, these results suggest that NFkB signalling is AKT-independent, occurring at more toxic levels and may be more important during non-homeostatic stress conditions. Furthermore, CKS1i co-treatment with NFkBi or AKTi (at 0.5 µM) further induced apoptosis on $CD45^+$ cells (Fig. 4i, j), decreasing live cell numbers (Suppl. Fig. 4m, n), after 4 days in OP9 co-culture. These results show that the CKS1-dependent AKT pathway is crucial for survival and proliferation of primitive LSK cells and suggests a positive NFkB-dependent stress-response feedback of CKS1i-treated LSKs.

Downstream of AKT activation, treatment with CKS1i (from 0.1 to 5 µM) resulted in increased Foxo1 phosphorylation at S256, a known AKT target site that leads to nuclear export[14], when compared to control (Fig. 4k, l and Suppl. Fig. 5a). Without changing total Foxo1 protein levels (Suppl. Fig. 5b). We observed decreased nuclear abundance of Foxo1 within KG1a cells treated with CKS1i and significant rescue at higher concentration (1 µM) when compared to lower concentration (0.1 µM) (Suppl. Fig. 5c, d), suggesting that induction of Foxo1 nuclear export by AKT-dependent phosphorylation in response to low doses of CKS1i. Furthermore, decrease in B cell numbers under CKS1i treatment is slightly rescued (non-significant) when co-treated with AKTi (1 µM) (Suppl. Fig. 5e, f), an effect that is not observed within $Ter119^+$ cells or $CD45^+$ population (Suppl. Fig. 5g, h). Finally, we observed that co-treatment of CKS1i with AKTi or NFkBi did not rescue cell survival or proliferation on ESLAM-HSCs under PVA expansion culture (Suppl. Fig. 5i, j). Together, these results demonstrate that tight regulation of intracellular kinase signalling cascades in HSCs is dependent on the SCF-SKP2-CKS1 complex and is responsible for modulating haematopoiesis, boosting differentiation at low dose of CKS1i via Foxo1-dependent mechanisms. Furthermore, high doses of CKS1i can activate the NFkB pathway, inducing toxicity to both the differentiation and proliferation potentials of HSCs.

266 **Discussion**

267 The study of pre-clinical agents to treat haematological disorders has largely focussed on
268 disease specific effects, with limited study of resident healthy haematopoiesis outside of
269 immediate/acute effects. This leaves a wide gap in our understanding of the long-term/late-
270 stage effects of novel chemotherapy on haematopoiesis, and has important implications for
271 efficient resource utilisation and the likelihood of clinical impact. Whereas the results of acute
272 treatment with CKS1i showing no effect on haematopoiesis *in vivo* are promising for CKS1i
273 tolerability by mature peripheral blood cells and bone marrow populations, studies such as
274 these do not model longer-term/late-stage effects of CKS1i on long-term haematopoiesis[8–10].

275 Previous studies have shown that complete loss of CKS1 functionality using a *Cks1*$^{-/-}$ mouse
276 model leads to sub-functional LT-HSC phenotypes, unable to engraft and repopulate the bone
277 marrow of irradiated mice[8,11]. In agreement, our data demonstrate that LT-HSCs are most
278 sensitive to CKS1 inhibition when forced to proliferate and without the protection of stromal
279 cells (Fig. 2). This result might be due to LT-HSCs in expansion culture[12] being more sensitive
280 to the cell cycle-targeting mechanism of CKS1i than when in differentiation cultures[13], which
281 are less proliferative[14,15]. Additionally, we demonstrate there is a differential threshold of
282 sensitivity to CKS1 inhibition during haematopoiesis, where erythropoiesis, a process known
283 to be highly dependent on consistent (and less specific) protein turnover[15], is much less
284 sensitive to CKS1 inhibition than B lymphopoiesis (Fig. 3d-h). We have previously
285 demonstrated that sensitivity to CKS1i correlates well with expression of the *CKS1B* gene
286 expression in AML cell lines[9], but our results show that the CKS1 degron in haematopoietic
287 cells is more representative of LT-HSCs and pre-B cells compared to pro-Erythrocytes using
288 CellRadar, and therefore functional responses do not necessarily correlate with *Cks1b* gene
289 expression alone (Fig. 4b and Suppl. Fig. 4a). These results suggest that single gene
290 expression does not predict cell type response of healthy haematopoiesis to drugs, and the
291 CKS1 degron has lineage specificity. We also observed higher sensitivity to CKS1i by all
292 myeloid populations (Suppl. Fig. 3m-q) grown with B lymphopoiesis-inducing cytokines when
293 compared to erythropoiesis-inducing cytokines. It is known that erythropoietin (EPO) used
294 within the ER condition can block apoptosis in erythrocytes[16], which may explain the overall
295 higher survival rate within the ER condition when compared to the B condition without EPO in
296 the culture, although this may not rescue apoptosis induced by high levels of CKS1i in the first
297 4 days. These results suggest a cytokine-specific response to CKS1i, however, the specific
298 effects of each individual cytokine from the *ex vivo* conditions on cell response to CKS1i still
299 need to be investigated. These results have major implications for the design of trials
300 combining CKS1 inhibition with cell cycle-cytotoxic chemotherapy such as Doxorubicin plus
301 Cytarabine (DA). We have previously shown that co-treatment is beneficial for LT-HSC

302 survival[9], but these data indicate that prolonged treatment may have negative effects on LT-
303 HSC recovery post-therapy and treatment should not out-last DA dosing regimens.

304 Interestingly, our data demonstrates that low doses of CKS1i boost all hematopoietic
305 populations analysed when LT-HSCs are subjected to multilineage differentiation, which is not
306 observed in AML cell lines (Fig. 3d and Suppl. Fig. 3j), showing a dose-dependent response
307 to CKS1i for *ex vivo* differentiation that contrasts with LT-HSC expansion. These results agree
308 with our previous study in human HSCs [9], and suggest novel functionalities for CKS1 within
309 healthy haematopoiesis, indicating tight regulation of CKS1-dependent protein degradation
310 induces proliferation within progenitor cells. Our proteomic analyses revealed the mechanism
311 underlying the bimodal CKS1i response in haematopoiesis via the AKT, NFkB and Foxo1
312 signalling pathways. We showed differential expression of protein regulators of AKT, NFkB
313 and Foxo1 in LSKs under CKS1i-treatment (Suppl. Fig. 4e). For example, CKS1i upregulates
314 the AKT regulator neuropilin (Nrp1), and Gsta4, a member of the glutathione s-transferase
315 family that induces lineage-biased haematopoiesis[17]. In contrast, CKS1i downregulates Ddp4
316 and Muc13, both regulators of the NFkB pathway, and overexpress Tab3, required for
317 maintenance of hematopoietic system[18]. Additionally, catalase (Cat), an indirect regulator of
318 NFkB has a role in regulating haematopoiesis *ex vivo*, either boosting transient expansion or
319 inducing quiescence of hematopoietic cells[19], and pirin (Pir), also a regulator of NFkB is
320 involved in regulation of cell differentiation during haematopoiesis[20]. These correspond to our
321 results showing that CKS1i-treatment can either boost haematopoiesis or halt proliferation of
322 LT-HSCs depending on culture conditions and treatment regimen. Furthermore, we
323 demonstrated an increase in pAKT/AKT and NFkB/IKBa levels within our LSKs treated with
324 apoptotic concentrations of CKS1i (Fig. 4e-h). It is known that AKT can regulate the
325 NFkB/IKBa axis and AKT phosphorylation of IKBa leads to proteasomal degradation and
326 subsequently release and translocation of NFkB to the nucleus, where it regulates pro-survival
327 genes. Conversely, stress-induced NFkB activation leads to IKBa phosphorylation[21], however,
328 AKT inhibition further increased abundance of NFkB, suggesting that NFkB activation is via a
329 stress response pathway, occurring at more toxic levels of CKS1i and may be less important
330 for boosting healthy haematopoiesis.

331 AKT is also important for phosphorylation of Foxo1, a key transcription factor regulating
332 haematopoiesis and particularly B lymphopoiesis[22,23]. Whereas under homeostasis, HSCs
333 have low AKT activity, regulating cycling via multiple targets, including Foxo1[14], stress can
334 over-activate AKT, inducing transient expansion of HSCs, eventually leading to their
335 exhaustion and finally depletion[24]. This dual role of AKT can be observed in our results, where
336 low doses of CKS1i leads to a boost in cell numbers (Fig. 3d) and high doses of CKS1i
337 deplete/exhaust all cells in culture (Fig. 3b-d). Furthermore, Foxo1 has been shown to

orchestrate B lymphopoiesis. During homeostasis Foxo1 levels fluctuate allowing for B cell lineage commitment and proliferation[22]. This may in part explain the high responsiveness of B lymphopoiesis to inhibition of CKS1 (Fig. 3g, h) and the heightened sensitivity of LT-HSCs and B cells to CKS1i compared to other progenitor cells (Fig. 4b). This also raises the important question of whether CKS1 would be a good target for treatment of B-lineage malignancies such as multiple myeloma [25,26], Burkitt lymphoma [27] and diffuse large B cell lymphoma [28], where it is overexpressed[27,28] and correlates with poor prognosis[25,26].

Altogether, these results begin to unravel the role of the CKS1/AKT/Foxo1 signalling axis on healthy haematopoiesis, suggesting that CKS1i-dependent AKT/Foxo1 activation/inhibition has a bimodal role in haematopoiesis, boosting levels at low CKS1i concentrations whilst completely ablating LT-HSCs at higher concentrations. In conclusion, we present a combination of rapid *ex vivo* culture systems to study long-term/late-stage effects of novel chemotherapeutic effects on haematopoiesis. Our results have particular relevance to the range of newer therapies with differing modes of action currently under development for AML. A major limiting factor of novel combination therapies under development is increasing haematopoietic toxicity leading to dosing interruptions and loss of clinical efficacy[29]. The ability to identify deleterious combinatorial effects early in the development process and selectively augment healthy haematopoiesis is of great potential utility. This system can be used to complement and, in time with additions, replace large, longitudinal animal studies and reveals cell-type specific and cytokine-specific effects of novel chemotherapeutic protocols.

Acknowledgments

We would like to acknowledge Karen Hogg and Graeme Park of the Biosciences Technology Facility at the University of York for flow cytometry sorting. We would like to thank Ellie Bennett for support with *in vivo* experimentation and the University of York Biological Service Facility. We would like to thank Chloë Baldreki of the MAPlab at the University of York for the proteomic sample preparation, and Zahra Masoumi for proteomics protocol development. We would like to thank William Critchley for support with experiment analysis.

References:

1. Sender, R. & Milo, R. The distribution of cellular turnover in the human body. *Nat Med* **27**, 45–48 (2021).

2. Shao, L. *et al.* Hematopoietic stem cell senescence and cancer therapy-induced long-term bone marrow injury. *Transl Cancer Res* **2**, 384–396 (2013).

3. Atallah, E. *et al.* Establishment of baseline toxicity expectations with standard frontline chemotherapy in acute myelogenous leukemia. *Blood* **110**, 3547–3551 (2007).

4. Kantarjian, H. *et al.* Intensive chemotherapy does not benefit most older patients (age 70 years or older) with acute myeloid leukemia. *Blood* **116**, 4422–4429 (2010).

5. Dombret, H. *et al.* International phase 3 study of azacitidine vs conventional care regimens in older patients with newly diagnosed AML with >30% blasts. *Blood* **126**, 291–299 (2015).

6. Pratz, K. W. *et al.* Long-term follow-up of VIALE-A: Venetoclax and azacitidine in chemotherapy-ineligible untreated acute myeloid leukemia. *Am J Hematol* **99**, 615–624 (2024).

7. Pollyea, D. A. *et al.* Outcomes in Patients with Poor-Risk Cytogenetics with or without TP53 Mutations Treated with Venetoclax and Azacitidine. *Clin Cancer Res* **28**, 5272–5279 (2022).

8. Grey, W. *et al.* The CKS1 / CKS2 Proteostasis Axis Is Crucial to Maintain Hematopoietic Stem Cell Function. *Hemasphere* **7(3)**, (2023).

9. Grey, W. *et al.* CKS1 inhibition depletes leukemic stem cells and protects healthy hematopoietic stem cells in acute myeloid leukemia. *Sci Transl Med* **3248**, (2022).

10. Grey, W. *et al.* The Cks1/Cks2 axis fine-tunes Mll1 expression and is crucial for MLL-rearranged leukaemia cell viability. *Biochim Biophys Acta Mol Cell Res* **1865**, 105–116 (2018).

11. Tomiatti, V. *et al.* Cks1 is a critical regulator of hematopoietic stem cell quiescence and cycling, operating upstream of Cdk inhibitors. *Oncogene* **34**, 4347–4357 (2015).

12. Wilkinson, A. C. *et al.* Long-term ex vivo haematopoietic-stem-cell expansion allows nonconditioned transplantation. *Nature* **571**, 117–121 (2019).

13. Safi, F. *et al.* In vitro clonal multilineage differentiation of distinct murine hematopoietic progenitor populations. *STAR Protoc* **4**, (2023).

14. Zhang, X., Tang, N., Hadden, T. J. & Rishi, A. K. Akt, FoxO and regulation of apoptosis. *Biochim Biophys Acta Mol Cell Res* **1813**, 1978–1986 (2011).

15. Chen, L. *et al.* Dynamic changes in murine erythropoiesis from birth to adulthood: implications for the study of murine models of anemia. *Blood Adv* **5**, 16–25 (2021).

16. Brines, M. & Cerami, A. Erythropoietin-mediated tissue protection: Reducing collateral damage from the primary injury response. *J Intern Med* **264**, 405–432 (2008).

17. Wang, L., Groves, M. J., Hepburn, M. D. & Bowen, D. T. *Glutathione S-Transferase Enzyme Expression in Hematopoietic Cell Lines Implies a Differential Protective Role for T1 and A1 Isoenzymes in Erythroid and for M1 in Lymphoid Lineages*. *Haematologica* vol. 85 (2000).

403 18. Takaesu, G. *et al.* TAK1 (MAP3K7) Signaling Regulates Hematopoietic Stem Cells through TNF-
404 Dependent and -Independent Mechanisms. *PLoS One* **7**, (2012).

405 19. Gupta, R., Karpatkin, S. & Basch, R. S. Hematopoiesis and stem cell renewal in long-term bone
406 marrow cultures containing catalase. *Blood* **107**, 1837–1846 (2006).

407 20. Licciulli, S., Cambiaghi, V., Scafetta, G., Gruszka, A. M. & Alcalay, M. Pirin downregulation is a
408 feature of AML and leads to impairment of terminal myeloid differentiation. *Leukemia* **24**,
409 429–437 (2010).

410 21. Yamamoto, Y. & Gaynor, R. B. IκB kinases: Key regulators of the NF-κB pathway. *Trends*
411 *Biochem Sci* **29**, 72–79 (2004).

412 22. Ushmorov, A. & Wirth, T. FOXO in B-cell lymphopoiesis and B cell neoplasia. *Seminars in*
413 *Cancer Biology* vol. 50 132–141 Preprint at https://doi.org/10.1016/j.semcancer.2017.07.008
414 (2018).

415 23. Lin, Y. C. *et al.* A global network of transcription factors, involving E2A, EBF1 and Foxo1, that
416 orchestrates B cell fate. *Nat Immunol* **11**, 635–643 (2010).

417 24. Wu, F., Chen, Z., Liu, J. & Hou, Y. The Akt–mTOR network at the interface of hematopoietic
418 stem cell homeostasis. *Exp Hematol* **103**, 15–23 (2021).

419 25. Zhan, F. *et al.* CKS1B, overexpressed in aggressive disease, regulates multiple myeloma
420 growth and survival through SKP2- and p27Kip1-dependent and -independent mechanisms.
421 *Blood* **109**, 4995–5001 (2007).

422 26. Chang, H. *et al.* Multiple myeloma patients with CKS1B gene amplification have a shorter
423 progression-free survival post-autologous stem cell transplantation. *Br J Haematol* **135**, 486–
424 491 (2006).

425 27. Keller, U. B. *et al.* Myc targets Cks1 to provoke the suppression of p27Kip1, proliferation and
426 lymphomagenesis. *EMBO Journal* **26**, 2562–2574 (2007).

427 28. Kratzat, S. *et al.* Cks1 is required for tumor cell proliferation but not sufficient to induce
428 hematopoietic malignancies. *PLoS One* **7**, (2012).

429 29. Short, N. J. *et al.* Azacitidine, Venetoclax, and Gilteritinib in Newly Diagnosed and Relapsed or
430 Refractory FLT3 -Mutated AML. *Journal of Clinical Oncology* **42**, 1499–1508 (2024).

431

432

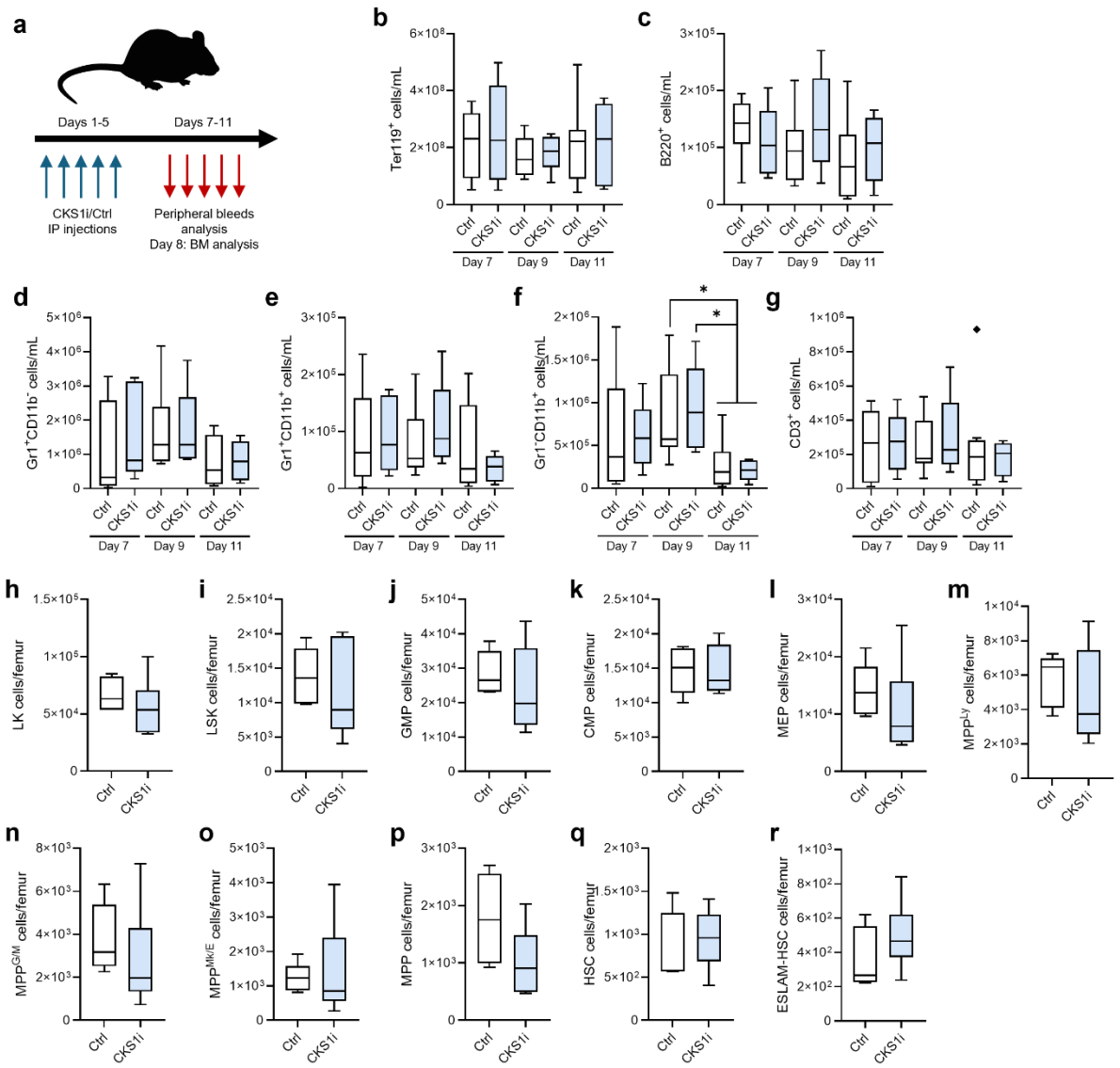

Figure 1. Acute *in vivo* effects of CKS1i on haematopoietic homeostasis. a. Schematic of CKS1i treatment (10 mg/kg) following peripheral blood or bone marrow analysis. Number of cells/mL of peripheral blood for b. Erythroid (Ter119+), c. B lymphoid (B220+), d-f. myeloid populations (Gr1+CD11b-, Gr1+CD11b+, Gr1-CD11b+) and g. T cells (CD3+), 2 (Day 7), 4 (Day 9) and 6 (Day 11) days post CKS1i treatment. Number of cells/femur for h. cKit+Sca1-Lineage- (LK), i. cKit+Sca1+Lineage- (LSK), j. granulocyte-monocyte progenitor (GMP: CD16/32+CD34+LK), k. common myeloid progenitor (CMP: CD16/32-CD34+LK), l. megakaryocyte-erythroid progenitor (MEP: LK/CD16/32-CD34-), m. multipotent progenitor with lymphoid bias (MPP^{Ly}: CD135+CD150-LSK), n. MPP with granulocytes and monocytes bias ($MPP^{G/M}$: CD135-CD48+CD150-LSK), o. MPP with megakaryocyte and erythroid potential ($MPP^{Mk/E}$: CD135-CD48+CD150+LSK), p. MPP with unbiased multilineage potential (CD135-CD48-CD150-LSK), q. HSC (CD135-CD48-CD150+LSK) and r. EPCR+ HSC (ESLAM-HSC) within the bone marrow of mice treated with vehicle control or CKS1i. White

447 indicates control, blue indicates CKS1i treated mice. N = minimum 5 per condition, statistical
448 significance was calculated by an Ordinary one-way ANOVA or Student's t-test, * = $p<0.05$.

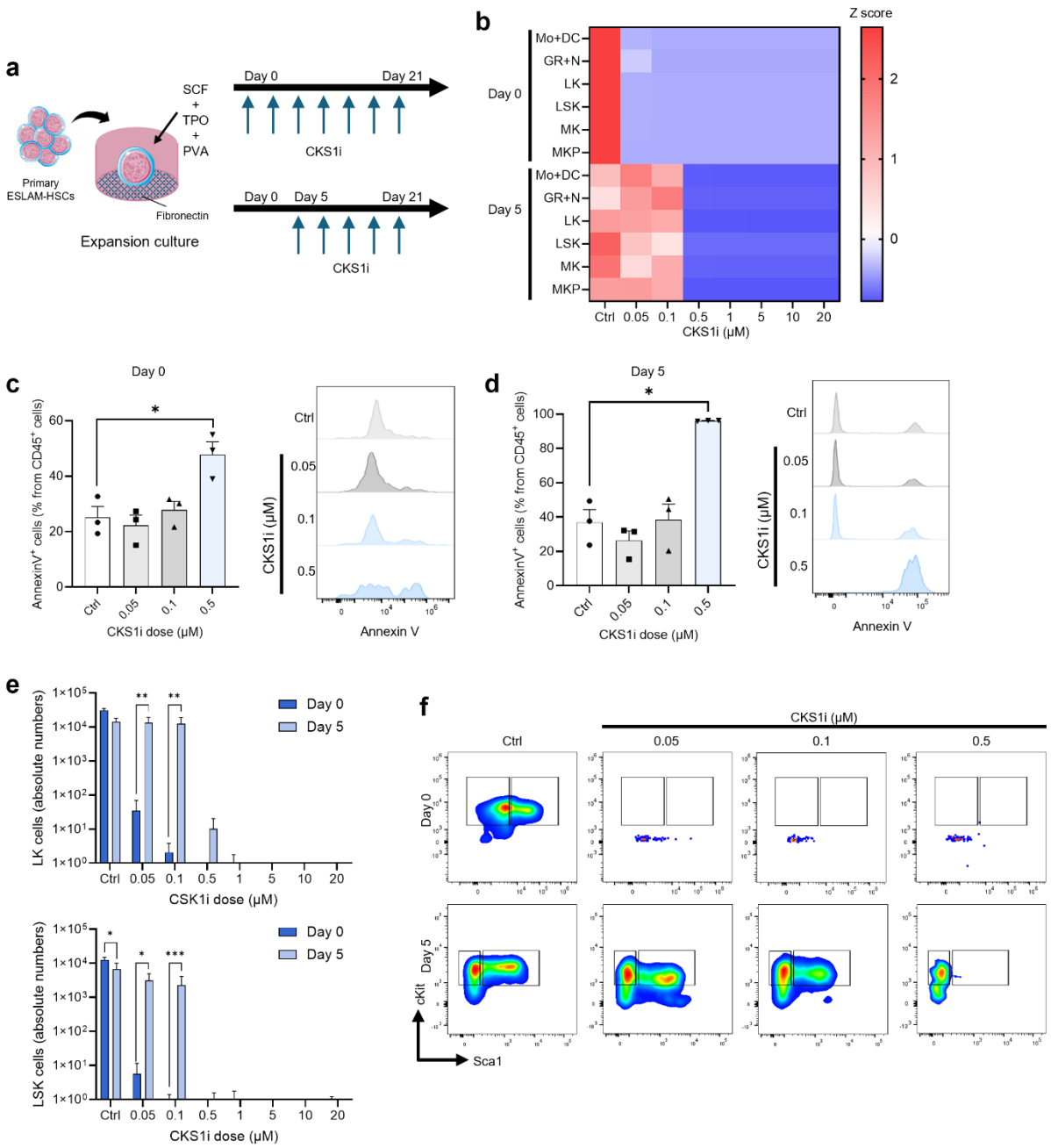

Figure 2. *Ex vivo* effects of inhibition of CKS1-dependent protein degradation on HSC expansion potential. a. Schematic of gold-standard PVA expansion culture system for 21 days indicating CKS1i treatment (0.05 – 20 μM) starting at Day 0 or Day 5. b. Heatmap depicting z scored expansion of the indicated immunophenotypic populations under control conditions and increased CKS1i dosage. Populations are defined as per Supp. Fig. 2a. Percentage of apoptotic (AnnexinV+) CD45+ cells after 4 days in expansion culture treated or not (Ctrl) with CKS1i from c. day 0 or d. day 5 in culture. e. and f. Absolute number and representative flow plots of LK and LSK cells treated with increasing dose of CKS1i from day 0 (dark blue) or day 5 (light blue). N = minimum 9 per condition, statistical significance was calculated by an Ordinary one-way ANOVA, * p<0.05, ** p<0.01, *** p<0.001.

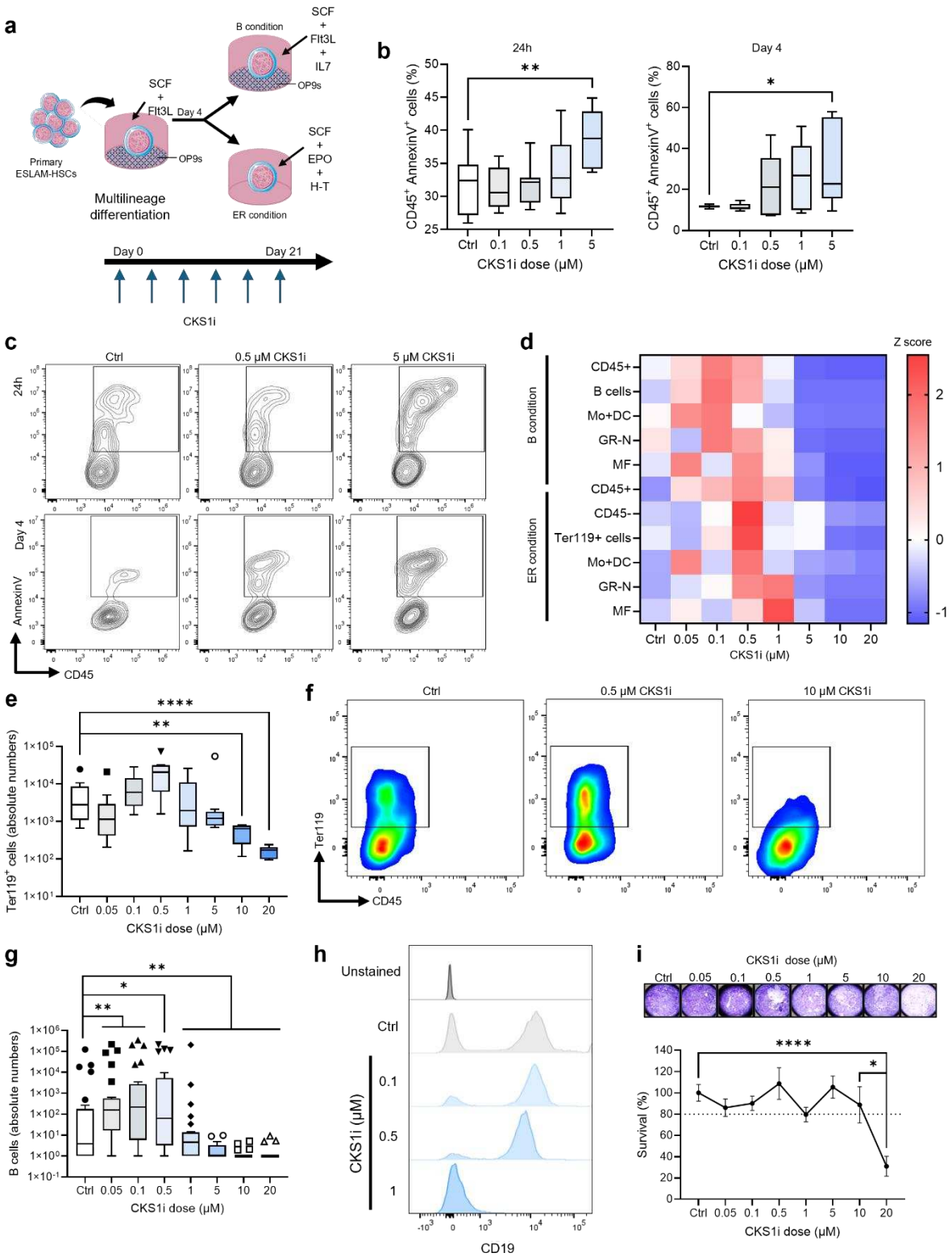

Figure 3. Multilineage differentiation reveals hematopoietic lineage-specific sensitivity to inhibition of CKS1-dependent protein degradation. a. Schematic of multilineage differentiation culture system treated with increasing doses of CKS1i. b. and c. Percentage of apoptotic (AnnexinV+) CD45+ cells and representative flow plots after 1- and 4-days treatment with increasing doses of CKS1i. d. Heatmap depicting z scored absolute number of the

466 indicated immunophenotypic populations (Supp. Fig. 3) under B lymphoid (FLT3L/IL7) and
467 Erythroid/Myeloid (EPO/H-T) differentiation conditions. e. and f. Absolute number and
468 representative flow plots of Ter119+ cells treated or not (Ctrl) with CKS1i. g. and h. Absolute
469 number and representative flow plots of B cells treated or not (Ctrl) with CKS1i. i. Crystal violet
470 measurement and representative images of OP9 stromal cell survival under increasing doses
471 of CKS1i for 21 days. N = minimum 9 per condition (except Annexin V assay, N = 6), statistical
472 significance was calculated by an Ordinary one-way ANOVA, * $p<0.05$, ** $p<0.01$, ****
473 $p<0.0001$.

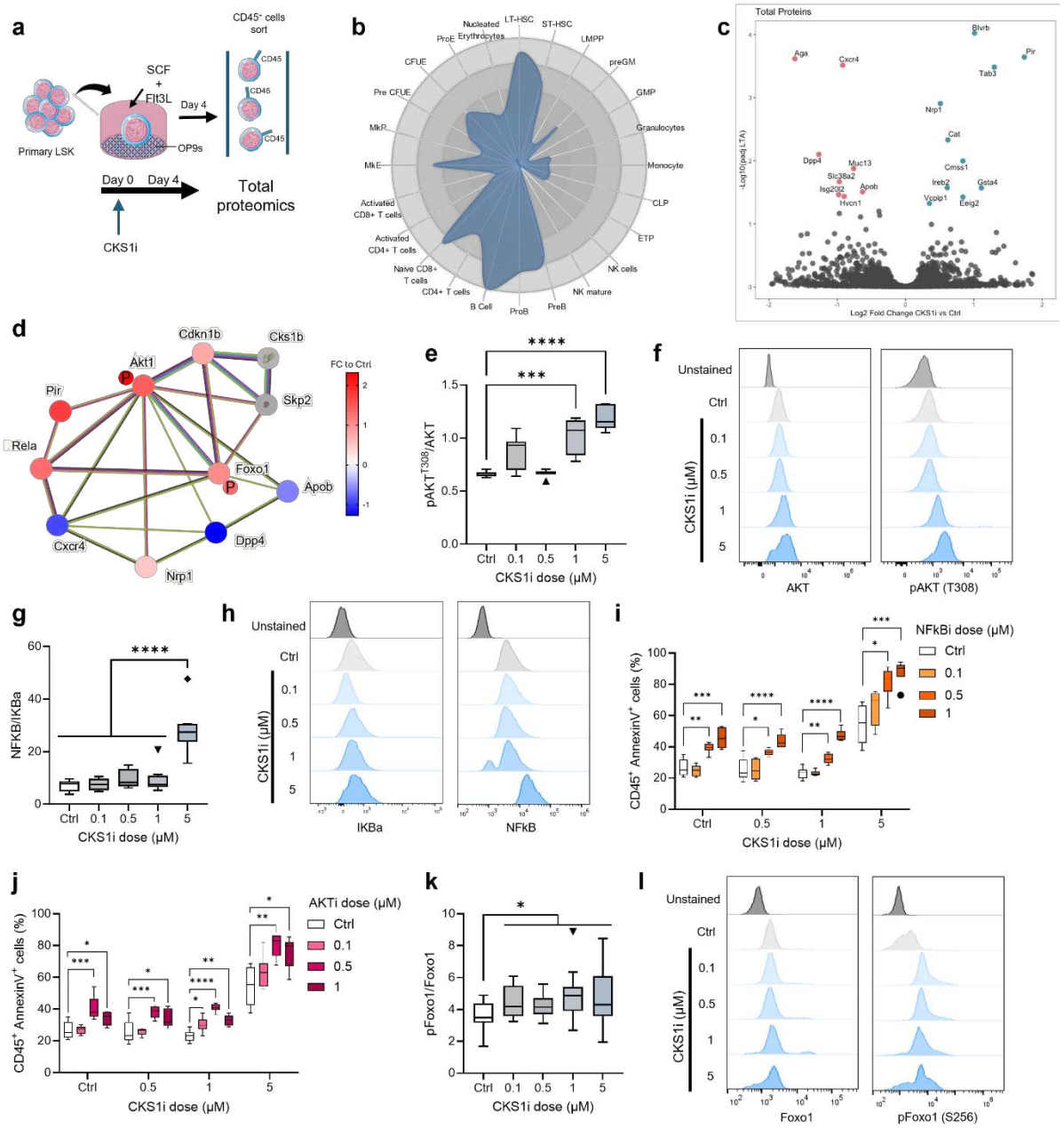

Figure 4. Total proteomics reveals mechanisms underlying primitive haematopoietic cells response to CKS1i. a. Schematic of 4-days LSK and OP9 co-culture treated or not (Ctrl) with CKS1i (1 μM) and CD45+ cell sorting for total proteomics. b. Mapping of differentially abundant proteins of hematopoietic cells under CKS1i-treatment to murine haematopoiesis (CellRadar). c. Volcano plot for CKS1i-treated vs Ctrl CD45+ cells after 4 days. Teal indicates significantly upregulated proteins, red indicates significantly downregulated proteins after CKS1i treatment. d. String network mapping signalling pathways activated on hematopoietic cells treated with CKS1i. e. and f. Ratio and representative flow plots of active pAKT (T308) to total AKT in CD45+ cells after 4 days treatment with CKS1i. g. and h. Ratio and representative flow plots of total NFkB to IKBa in CD45+ cells treated or not with CKS1i. Percentage of apoptotic (AnnexinV+) CD45+ cells treated with combination of CKS1i and i.

486 NFkBi or j. AKTi for 4 days. k. and l. Ratio and representative flow plots of total Foxo1 to active
487 pFoxo1 (S256) in CD45+ cells treated with CKS1i. N = minimum 6 per condition, statistical
488 significance was calculated by an Ordinary one-way ANOVA, * $p<0.05$, ** $p<0.01$, *** $p<0.001$,
489 **** $p<0.0001$.

490

491

492 **Supplementary Materials**

493 **Extended methods**

494 *Cell culture*

495 OP9 stromal cells were cultured in Opti-MEM with 10% fetal bovine serum (FBS), 1%
496 penicillin/streptomycin (P/S) and 0.1% 2-marcaptoethanol (complete Opti-MEM; Thermo
497 Fisher Scientific). AML cell lines THP1 and KG1a were cultured in RPMI 1640 medium
498 (Thermo Fisher Scientific) with 10 or 20% FBS, respectively, and 1% P/S.

499 *Primary bone marrow cell isolation*

500 Primary murine bone marrow cells were isolated by crushing the bones in FACS buffer
501 (phosphate-buffered saline, PBS, with 2% FBS), followed by red blood cell lysis for 5 mins on
502 ice before lineage marker positive cell-depletion using the hematopoietic progenitor cell
503 isolation kit following the manufacturer's instructions (StemCell Technologies, CAT#133311).

504 *Flow cytometry and cell sorting*

505 Cells in culture or bone marrow cells were stained with antibodies indicated in Supplementary
506 Table 1 in FACS buffer for 30 min on ice in the dark and acquired on a BD LSRFortessa flow
507 cytometer (BD Biosciences) or sorted on a MoFlo Astrios (Beckman Coulter). Cell viability and
508 apoptosis were assessed by Annexin V-FITC apoptosis detection kit (BD Biosciences) and
509 DAPI (10 µg/ml; Generon) following the manufacturer's instructions. For phosphoprotein flow
510 cytometry, cells were initially stained with surface marker (Supplementary Table 1) and DAPI
511 for 30 min on ice in the dark and washed three times with FACS buffer before fixation using
512 BD Cytofix/Cytoperm followed by permeabilization using BD Phosflow Perm III buffer (BD
513 Biosciences) following the manufacturer's instructions. Cells were stained with intracellular
514 antibodies overnight at 4°C in the dark and washed 4 times with FACS buffer before analysis
515 on CytoFLEX LX (Beckman Coulter). All flow cytometry data was analysed using FlowJo
516 software.

517 *Microscopy*

518 KG1a cells were resuspended in PBS and centrifuged at 800 rpm for 5 minutes using a
519 Cytospin 4 (Thermo Fisher Scientific) before immunostaining following the manufacturers
520 protocol for FoxO1 (C29H4; Cell Signalling) immunofluorescence. The cells were imaged
521 using a ZEISS Elyra 7 microscope and images analysed using ImageJ and ZEISS ZEN 3.1
522 software.

523 *Statistical analysis*

524 Proteomic data was initially analysed using FragPipe (frag-pipe-analyst.org) with a false
525 discovery rate (Benjamini Hochberg) of <0.05 and log2 fold change of +/-0.5 called as
526 significant. Flow cytometry data was analysed using GraphPad Prism software with the
527 indicated n and statistical tests detailed in each figure legend.

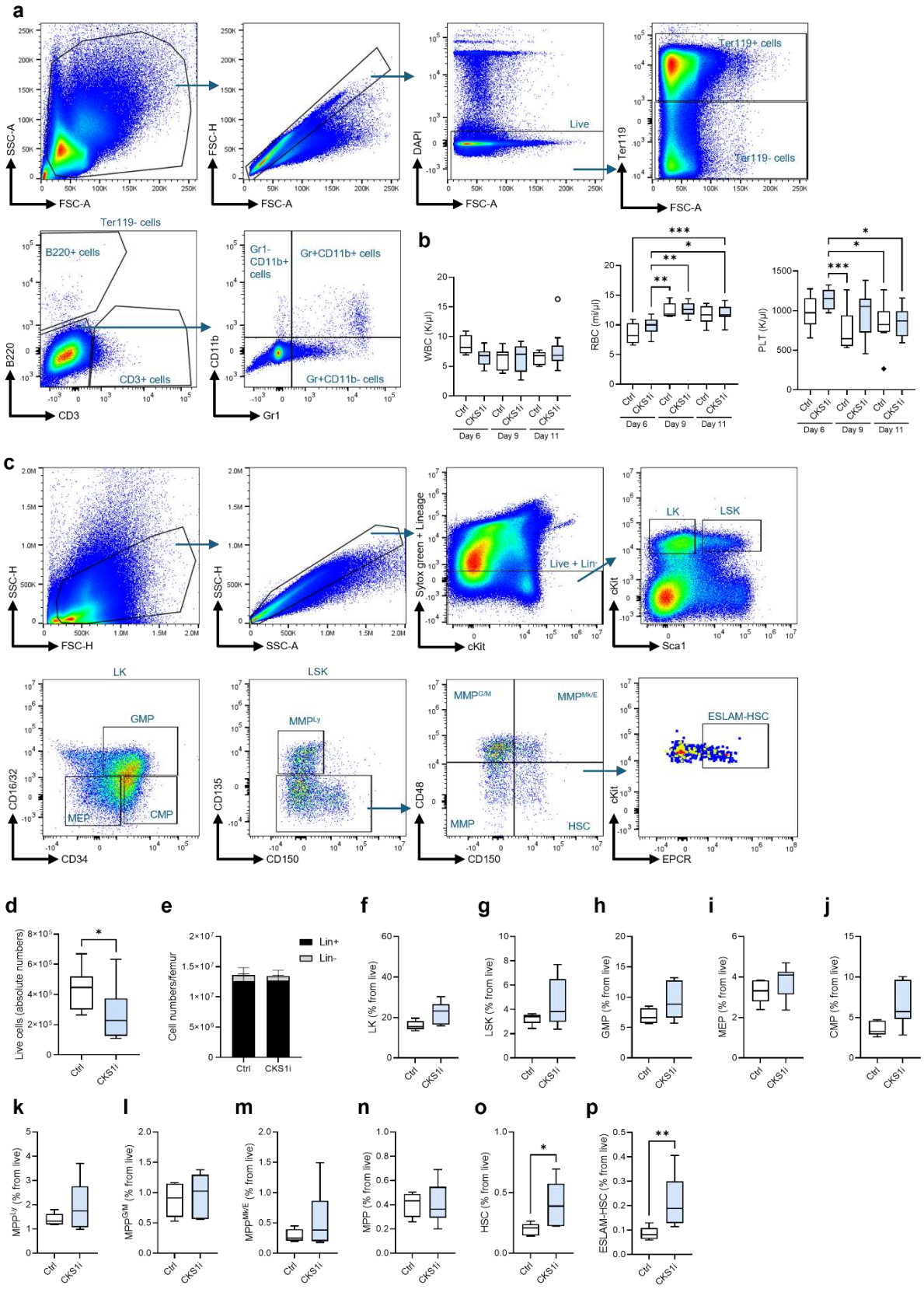

Supplementary Figure 1

Supplementary Figure 1. a. Gating strategy for peripheral blood analysis. b. White blood cell (WBC), red blood cell (RBC) and platelet (PLT) counts of vehicle treated control (Ctrl) versus CKS1i-treated (CKS1i) mice. c. Gating strategy for bone marrow populations analysis. d. Total bone marrow live cell numbers from control compared to CKS1i-treated mice. e. Lineage positive (Lin+) and negative (Lin-) cell numbers per femur of mice treated with CKS1i or vehicle control. Percentage from live cells of f. cKit+Sca1-Lin- (LK), g. cKit+Sca1+Lin- (LSK), h. granulocyte-monocyte progenitor (GMP: cKit+Sca1-CD16/32+CD34+Lin-), i. megakaryocyte-erythroid progenitor (MEP: cKit+Sca1-CD16/32-CD34-Lin-), j. common myeloid progenitor (CMP: cKit+Sca1-CD16/32-CD34+Lin-), k. multipotent progenitor with lymphoid bias (MPP^{Ly}: cKit+Sca1+CD135+CD150-Lin-), l. MPP with granulocytes and monocytes bias ($MPP^{G/M}$: cKit+Sca1+CD135-CD48+CD150-Lin-), m. MPP with megakaryocyte and erythroid potential ($MPP^{Mk/E}$: cKit+Sca1+CD135-CD48+CD150+Lin-), n. MPP with unbiased multilineage potential (cKit+Sca1+CD135-CD48-CD150-Lin-), o. HSC and p. EPCR+ HSC (ESLAM-HSC) within the bone marrow of mice treated with vehicle control or CKS1i. White indicates control, blue indicates CKS1i treated mice. N = minimum 5 per condition, statistical significance was calculated by an Ordinary one-way ANOVA or Student's t-test, * = $p<0.05$, ** = $p<0.005$, *** = $p<0.0005$.

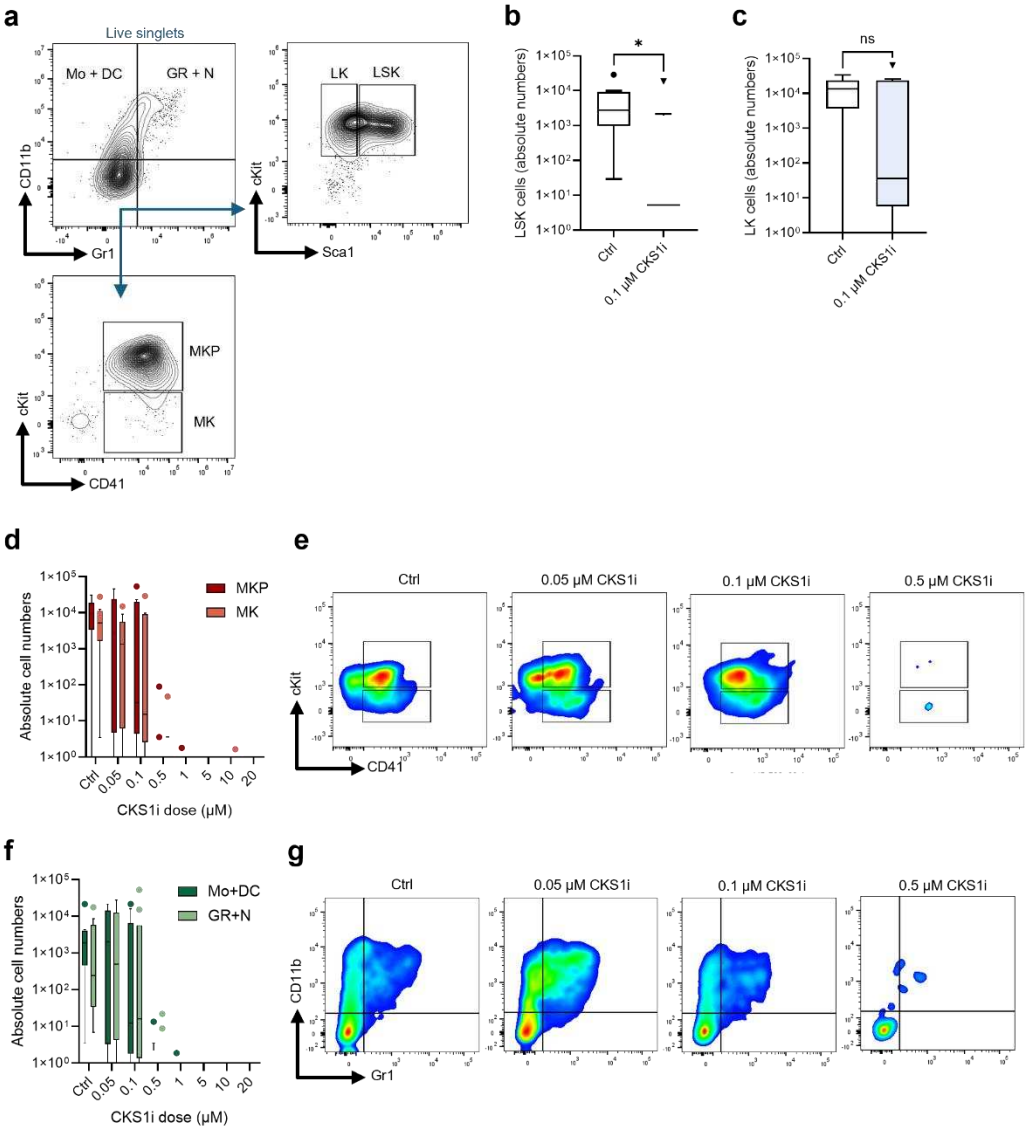

Supplementary Figure 2.

547

548 **Supplementary Figure 2.** a. Immunophenotyping of post-PVA expansion culture. b. Absolute
549 number of LSK cells comparing untreated control (Ctrl) to 0.1 µM CKS1i treatment. c. Absolute
550 number of LK cells comparing control to 0.1 µM CKS1i treatment. d. and e. Absolute number
551 and representative flow plots of Megakaryocyte progenitors (MKP) and Megakaryocytes (MK)
552 in response to increasing doses of CKS1i. f. and g. Absolute number and representative flow
553 plots of Monocytes + Dendritic cells (Mo+DC) and Granulocytes + Neutrophils (GR+N) in
554 response to increasing doses of CKS1i. N = minimum 9 per condition, statistical significance
555 was calculated by an Ordinary one-way ANOVA, * $p<0.05$.

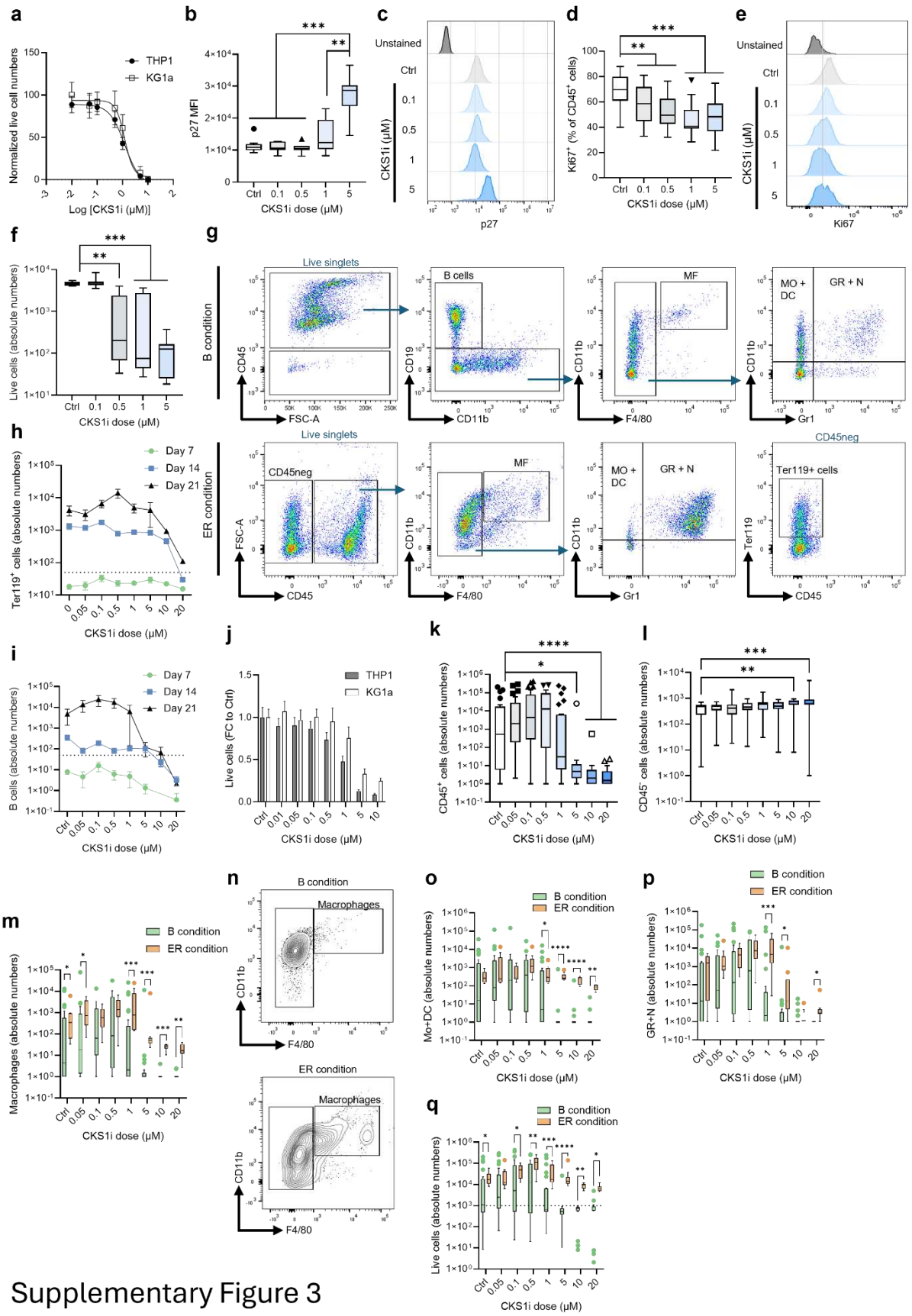

Supplementary Figure 3

Supplementary Figure 3. a. IC50 of AML cell lines THP1 and KG1a treated with CKS1i. b. and c. Abundance and representative flow plots of p27 within LSKs treated for 4 days with CKS1i. d. and e. Percentage and representative flow plots of Ki67+ CD45+ cells after 4 days treatment with CKS1i. f. Live cell numbers of LSKs in 4-days co-culture with OP9s treated with CKS1i. g. Gating strategy for endpoint analysis of multilineage differentiation cultures. Absolute h. Ter119+ cell and i. B cell numbers at days 7, 14 and 21 of multilineage differentiation protocol. j. Absolute live cell numbers of AML cell lines THP1 and KG1a treated with CKS1i. Absolute number of k. CD45+ and l. CD45- cells in response to increasing doses of CKS1i under B lymphoid conditions. m. and n. Comparison of macrophage (MF) numbers and representative flow plots within B lymphoid (B) and Erythroid/Myeloid (ER) conditions. Comparison of o. Monocyte and Dendritic cell (MO + DC) and p. Granuloctye and Neutrophil (GR + N) numbers within B or ER condition. q. Absolute live cell numbers comparison between B and ER conditions. N = minimum 9 per condition, statistical significance was calculated by an Ordinary one-way ANOVA, * $p<0.05$, ** $p<0.01$, *** $p<0.001$, **** $p<0.0001$.

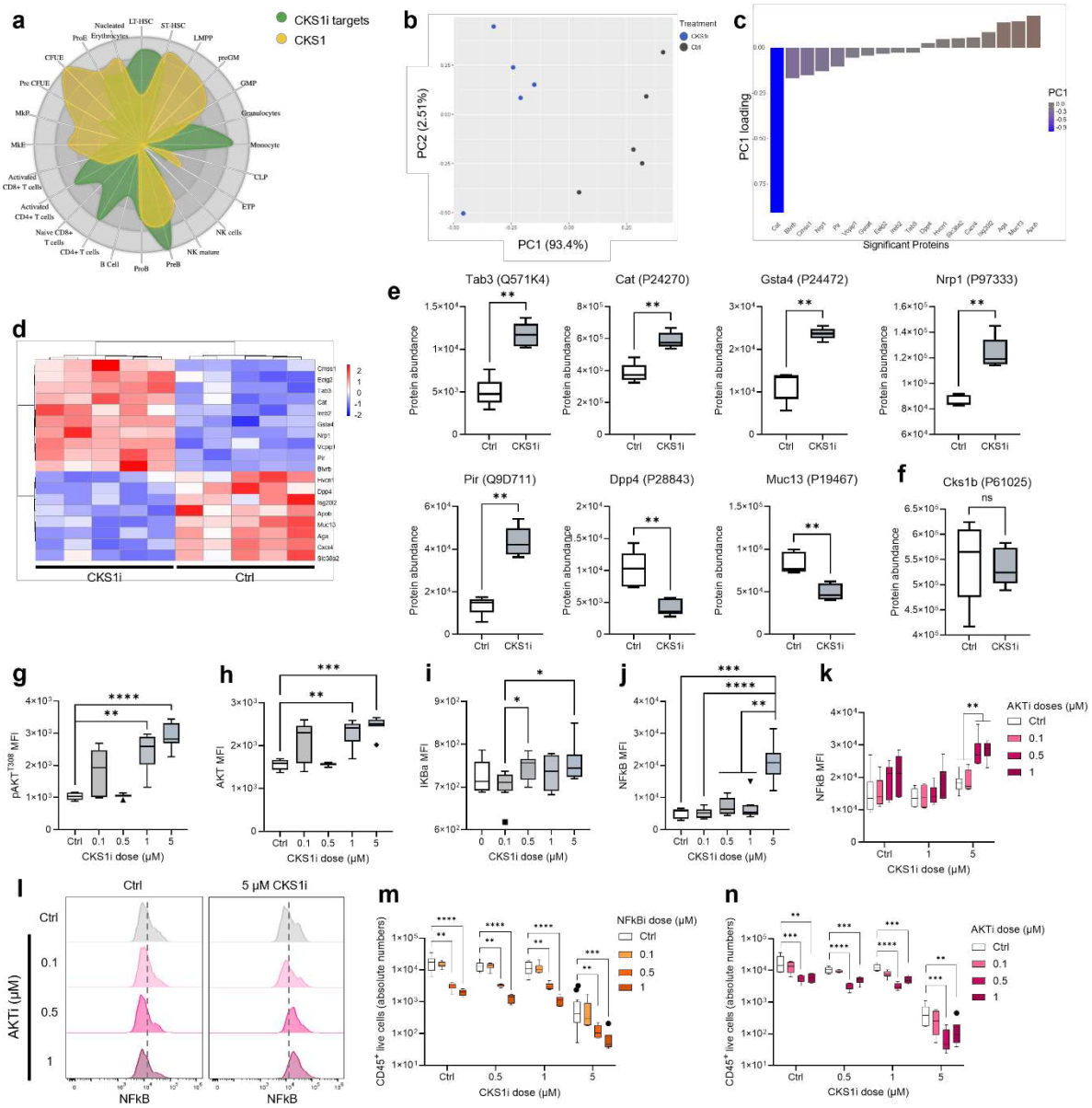

Supplementary Figure 4.

576 **Supplementary Figure 4.** a. Mapping of CKS1 alone and CKS1i targets identified in human
577 HSPCs[11] to haematopoiesis (CellRadar). b. Principal component analysis of significantly
578 different proteins between untreated control (Ctrl) and CKS1i treated $CD45^+$ cells. c. PC1
579 loadings for a. d. Heatmap of differentially abundant proteins between Ctrl and CKS1i treated
580 CD45+ cells. e. Differentially abundant proteins in CKS1i treated cells mapping to Foxo1 and
581 NFkB regulation. f. Protein abundance of CKS1 in CD45+ cells treated or not with CKS1i.
582 Abundance of g. active pAKT (T308), h. total AKT, i. total IKBa, j. total NFkB in CD45+ cells
583 in response to increasing doses of CKS1i. k. and l. Abundance and representative flow plots
584 of NFkB in CD45+ cells in response to CKS1i co-treatment with AKTi. Absolute live cell
585 numbers of CD45+ cells co-treated with CKS1i and m. AKTi or n. NFkBi for 4 days. N =
586 minimum 6 per condition, statistical significance was calculated by an Ordinary one-way
587 ANOVA, * $p<0.05$, ** $p<0.01$, *** $p<0.001$, **** $p<0.0001$.

588

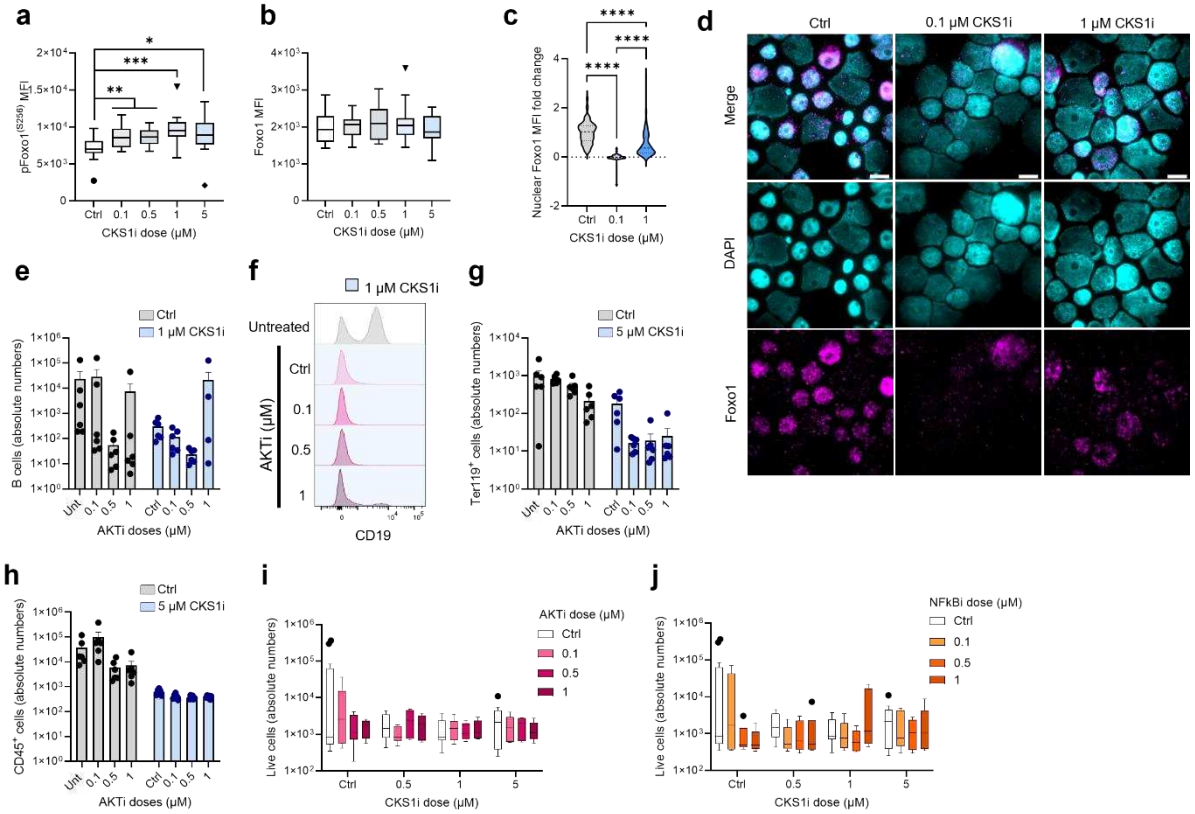

Supplementary Figure 5.

589

590 **Supplementary Figure 5.** Abundance of a. active pFoxo1 (S256) and b. total Foxo1 within
591 $CD45^+$ cells treated or not with CKS1i. c. and d. Fold change abundance and representative
592 microscopy images of nuclear Foxo1 in KG1a treated or not with CKS1i. Cyan represents
593 DAPI staining and fuchsia represents Foxo1 staining. e. and f. Absolute number and
594 representative flow plots of B cells (CD19+) treated or not (Unt: untreated) with combination
595 of CKS1i and AKTi within 21 days differentiation culture. Absolute number of g. Ter119+ cells
596 and h. CD45+ cells treated or not (Unt) with combination of CKS1i and AKTi within 21 days
597 differentiation culture. Live cell numbers of ESLAM-HSCs within 21-days PVA expansion
598 culture co-treated with i. CKS1i and AKTi or j. CKS1i and NFkBi. N = minimum 6 per condition,
599 statistical significance was calculated by an Ordinary one-way ANOVA, * $p<0.05$, ** $p<0.01$,
600 *** $p<0.001$, **** $p<0.0001$.

601 **Supplementary Table 1.**

Reagent or resource	Source	Identifier
Antibodies (flow cytometry)		
Annexin V apoptosis detection kit	BD Biosciences	556547
Anti-mouse lineage cocktail	Biolegend	133311
AKT (pT308)	BD Biosciences	558275
AKT total	Cell signalling	5186S
B220	Biolegend	103236
CD3	Biolegend	100206
CD11b	BD Biosciences	557657
CD19	Biolegend	152418
CD41	Biolegend	133915
CD45	Biolegend	103108
CD45.2	Biolegend	109824
CD48	Biolegend	103438
CD150	Biolegend	115914
cKit	Biolegend	105826
EPCR	eBioscience	15228719
F4/80	Biolegend	123116
Foxo1 (pS256)	Online AB	ABIN684755
Foxo1 (C29H4) Rabbit mAb	Cell signalling	2880S
Foxo1 total	Cell signalling	14262S
Goat anti-Rabbit AF647	Proteintech	RGAR005
Gr1	Biolegend	108408
IkBa	Cell signalling	8993S
Ki67	BD Biosciences	563756
NFkB (p65)	Cell signalling	49445S
p27	Cell signalling	12184S
Sca1	Biolegend	108128
Ter119	Biolegend	116222
DAPI	Generon	40043
Sytox green	Fisher Scientific	10768273
Chemicals, peptides and recombinant proteins		
AKT inhibitor - MK-2206 2HCl	Selleckchem	S1078
2-Mercaptoethanol	Fisher Scientific	31350010
BD Cytofix/Cytoperm	BD Biosciences	554714
BD Phosflow Perm III buffer	BD Biosciences	558050
CKS1 inhibitor	Merck	432001-69-9
Crystal violet	VWR International	911517ZA
DMEM/F12	Fisher Scientific	1056518
FBS	Fisher Scientific	16000044
Fibronectin	Fisher Scientific	10526961
HEPES	Fisher Scientific	15630049
hEPO	Stemcell Tech	78007.1
hHoloTransferrin	Merck	T0665
hIL7	Proteintech	HZ-1281
ITS-X	Fisher Scientific	10524233
L-glutamine	Appleton Woods	10-016-CV
mFlt3L	Peprotech	250-31L
mSCF	Peprotech	AF-250-03
mTPO	Peprotech	315-14
NFkB inhibitor -TPCA-1	APExBIO	A4602
Opti-MEM	Fisher Scientific	12559099
P/S	Fisher Scientific	11548876
ProLongTM Gold antifade reagent	Invitrogen	P36934
PVA	Merck	P8136
RPMI 1640	Fisher Scientific	11875093
StemSpan	Stemcell Tech	9600
Software, algorithms and data availability		
FlowJo v10.6.1	FlowJo	N/A

ImageJ	National Institute of Health	N/A
Prism 7	GraphPad	N/A
CellRadar	https://karlssong.github.io/cellradar/	N/A
ZEISS ZEN 3.1	ZEISS	N/A

Supplementary Table 2: Liquid chromatography-mass spectrometry data by Cambridge (DIA)-NN software against the mouse reference.

Graphical Abstract